EXPERIMENTAL VERIFICATION OF TURBULENCE MODELING FOR THE FLOW THROUGH A POROUS MEDIA BY USING PTV

Sota Nakajo
Disaster Prevention Research Institute
Kyoto University
Uji Gokasho, Kyoto, 611-0011, Japan
nakajo@oceanwave.jp

Takaaki Shigematsu
School of Engineering
Osaka City University
3-138, Sugimoto-3, Sumiyoshi-ku, Osaka, 558-8585, Japan
shige@urban.eng.osaka-cu.ac.jp

ABSTRACT

Distribution of turbulent properties in a porous media has not been clear at all. Therefore most of existing turbulence models for a porous media flow which many researchers have proposed were macroscopic models based on the knowledge of pressure drop along a porous media. In the present study, we validated a linear and a nonlinear turbulence models by a priori testing based on the measurement data of velocity inside a porous media using a high resolution PTV with the refractive index matching method. As a result, it was cleared that a nonlinear turbulence model with nonlinear velocity gradient agree to the experimental results much better than a linear turbulence model for the flow passing through a porous media. Moreover, it was presented that the coefficient in the nonlinear model is constant and independent with the Reynolds number and spatial averaging area size.

BACKGROUND AND MOTIVATION

The continuous study of the flow passing through a porous media following the pioneering work of Darcy (1856) for the low-speed seepage flow has investigated for a long time. To this day, the knowledge of a porous media flow is pursued in widespread engineering field, for example, chemical, mechanical, nuclear, groud water, hydraulics and environment engineering and so on. Especially, the porous media flow turn to turbulence regime at relatively low Reynolds number condition in comparison with the clear flow (Jolls and Hanratty, 1964; Dybbs and Edwards, 1984). Therefore, microscopic measurement and modeling of turbulence is essential in order to elucidate the process of mass and heat transfer and energy loss in a porous media.

However, there are few measurement researches of fluid velocity in a porous media because of the difficulty caused by the 3-D coomplex aperture geometry and invisibility. The fact led to the development of macroscopic turbulent models based on the relationship between bulk flow velocity and pressure drop (Masuoka and Takatsu, 1996; Antohe and Lage, 1997; Nakayama and Kuwahara, 1999; Pedras and de Lemos, 2001; Teruel and Rizwan-uddin, 2009). Nevertheless, almost all these models based on the assumption that turbulent stress have linear correlation with shear velocity. And there has been few information to deceide whether this assumption is correct or not so far.

On the other hand, the Refractive Index Matching Method (RIMM) shed a ray of light on the study of the porous media flow. For the first time, Jolls and Hanratty (1964) observed the transition of flow regimes by using dye visualization with a porous media model and fluid which had same refractive index in the experiment. After that, Dybbs and Edwards (1984) conducted asynchronous multipoint measurement of time series of velocity by Laser Doppler Anemometer with RIMM. Recently, simultaneous multipoint measurement by Particle Image Velocimetry with RIMM was available for the progress of a high-speed camera and some studies using this method were presented (Saleh *et al*., 1992, Dill *et al*., 1995). However, these research presented only methodology and no significant information concern with turbulence in a porous media. Exceptionally, Yevseyev *et al*. (1991) measured turbulent intensity distribution in a porous media by LDA with RIMM.

With this background, Nakajo *et al*. (2008) carried out measurement of velocity distribution inside and around a porous media with high resolution in time and space by Particle Tracking Velocimetry which is a type of PIV with RIMM and examined the relation between approach velocity and turbulent energy generated in a porous media settled in unidirectional flow. In present study, we focused attention on the detail of relationship between turbulent stress and velocity gradient terms by using measurement data and verification of turbulence modeling for the flow passing through a porous media.

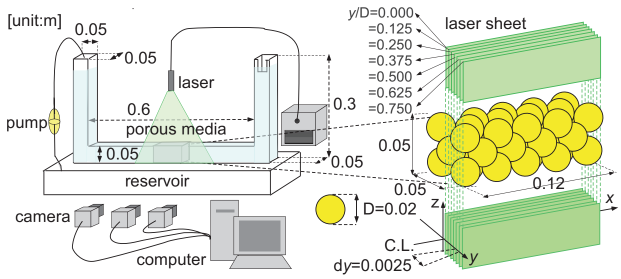

Figure 1. Experimental apparatus

Table 1: Experimental conditions

D [m]	ϕ	ϕD [m]	V_0 [m/s]	Re_p
0.010	0.32	3.2×10^{-3}	0.021	75
			0.029	103
			0.043	153
0.020	0.45	9.0×10^{-3}	0.020	200
			0.026	260
			0.032	320
			0.040	400
			0.052	520
0.025	0.53	1.3×10^{-2}	0.021	309
			0.036	530
			0.044	648

METHOD

The flow passing through a complicated aperture has a strong unsteadiness. Therefore, turbulence modeles based on spatial averaging approach are treated in this study.

In many turbulence model, the Reynolds stress is propotional to the gradient of averaged velocity, γ_{ij} and the eddy viscosity ν_t is introduced as the proportional constant.

$$Rs_{ij} = \frac{2}{3}\delta_{ij}k - 2\nu_t\gamma_{ij} \tag{1}$$

$$\gamma_{ij} = \frac{1}{2}\left(\frac{\partial v_i}{\partial x_j} + \frac{\partial v_j}{\partial x_i}\right) \tag{2}$$

where v_i is a spatial averaged velocity component in i direction, k is turbulence energy and δ_{ij} is the Kronecker's delta function. In this model as sometimes called the eddy viscosity model, ν_t is considered to have a positive value in general. That is to say that signs of turbulent stress and shear velocity have to be same. Neverthless, actual measurement results shows this consideration is not necessarily justifyed.

According to Piomelli *et al.* (1988), methods of verification of turbulence model are classified into two groups. One is to simulate target flow and then compare the results with experimental data (*a posteriori* model testing). Another is to compare the local instantaneous turbulent stress got from fully resolved velocity field data with the prediction of model (*a priori* model testing). With the latter method, Clark *et al.* (1979) analyzed sub-grid turbulent stress from DNS results for periodic homogeneous isotropic turbulence and compare it with the prediction obtained by substituting mean flow information into the Smagorinsky model formulated by the following equation :

$$\nu_t = (C_s\lambda)^2\sqrt{2\gamma_{ij}\gamma_{ij}} \tag{3}$$

where λ is a turbulent length scale and identified a spatial filter scale generally. C_s is a model coefficient. As a result, they presented reproduced the reproduced turbulent stress calculated the Smagorinsky model had very little correlation with the actual stress.

Instead of DNS results, high resolution PIV data is able to use for validation of turbulent models. For example, Liu *et al* (1994) measured turbulent jet flow by PIV and verified the Smagorinsky model. They also concluded that the Smagorinsky model is not appripriate to reproduce the actual stress distribution. On the other hand, they showed another simple turbulence model.

$$Rn_{ij} = C_n\lambda^2 A_{ik}A_{jk} \tag{4}$$

where A_{ik} is a velocity gradient term, $\partial v_i/\partial x_k$, and C_n is a model coefficient. They deduced this turbulence model from the Taylor expansion of velocity component and scale simillality model. This model was called a nonlinear model and showed the relatively high correlation between observation and prediction.

In this study, we conducted *a priori* testing of the eddy viscosity model and the nonlinear model based on high resolution PTV data. The turbulent components were defined by spatial averaging and decomposition as :

$$\langle v\rangle = \frac{1}{V_f}\int_{V_f} v_m dv \tag{5}$$

$${}^i v = v_m - \langle v\rangle \tag{6}$$

where v_m is a measured velocity and V_f is a volume of fluid in spatial averaging area. Bracket $\langle\ \rangle$ denotes spatial-averaged value and ${}^i v$ is a turbulent component. Then turbulent stress R_{ij} was defined by the following equation.

$$R_{ij} = \frac{1}{V_f}\int_{V_f} {}^i v_i {}^i v_j dv \tag{7}$$

In previous *a priori* testing studies, spatial correlation-based PIV algorithm was used for velocity measurement (Liu *et al.*, 1994; Tao *et al.*, 2002). However, the PIV algorithm includes a spatial filter in analysis principle itself. That is to say that this method is inadequate for the definition of turbulence by spatial averaging procedure. Therefore, a high-resolution PTV algorithm (Super-resolution KC method; Takehara *et al.*, 2000) was adopted in this study.

A series of experiment was conducted using a rectangle flume with 0.6m horizontal length, 0.05m height and 0.05m width (**Figure 1**). The both ends of horizontal part were jointed to a vertical pipe with square cross section. Unidirectional flow was made by pumping fluid up into a vertical pipe from a reservoir tank and overflowing freely from the other vertical section. Porous media model was fixed at the center of flume. In this study, we used the RIMM developed by Etoh *et al*. (1996) for getting undistorted images in a porous media. In order to match the refractive index of fluid and porous media model, approximately 40 weight percent of iodide sodium solution and clear silicon spheres were used respectively. 1024 images were captured by three high-speed cameras during approximately 4.1 seconds with 250fps respectively. In order to shine on tracers, a laser light sheet was irradiated from the top of the horizontal section along the longitudinal axis of the flume. 2D velocity field information was obtained using this method. In order to recognize the difference of measurement section, we got images every 0.025m in perpendicular to the x-axis by sliding a laser light sheet. Three types of porous media models were prepared in order to consider the influence of pore scales ϕD (ϕ : porosity, D : diameter of silicon spheres). Details of experimental condition were presented in **Table 1**. In this table, V_0 is an approaching velocity. Mean density of measured velocity vectors was approximately 230 per cm^2. The governing parameter, the Reynolds number R_{ep} was defined as :

$$R_{ep} = \frac{\phi D V_0}{\nu} \tag{8}$$

where ν is a kinematic viscosity coefficient of the fluid used in the experiment (ν=0.9×10^{-6}m^2/s).

As a preliminary experiment, the simpler and elementary flow around a single cylinder was measured using the same experimental apparatus. The cylinder diameter was $D = 0.017$m and the Reynolds number was $R_e = DV_0/\nu = 700$. This Reynolds number was relatively low, but the unsteady flow was observed behind the cylinder.

In order to estimate turbulent stress by using equation (4), three dimensional velocity gradient information was necessary. However, only 2D velocity field information obtained by this experiment was available. The equation (4) is rewritten using shear velocity γ_{ij}, rotational velocity ω_{ij} and strain velosity ε_i as :

$$Rn_{ij} = \frac{C_n\lambda^2}{2}\left\{\gamma_{ij}(\varepsilon_i+\varepsilon_j) - \omega_{ij}(\varepsilon_i-\varepsilon_j) + \frac{1}{2}(\gamma_{ik}-\omega_{ik})(\gamma_{jk}+\omega_{jk})\right\} \tag{9}$$

Final term was omitted from calculation in this study bacause the velocity gradient with k direction was not obtained. This omission was easily acceptable in a preliminary experiment since the dominant flow was 2D. The discussion for the porous media flow was shown at subsequent section. A characteristic length of turbulent eddy was set as $\lambda = \ell^{2/3}$ (ℓ is a radius of spatial averaging) on ground that 3D turbulence was modeled from 2D measurement data.

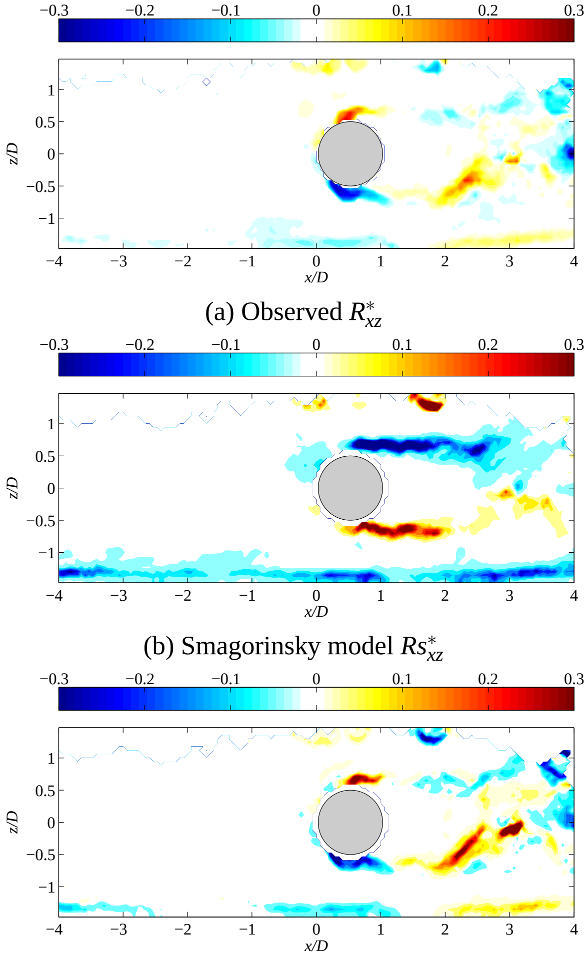

(c) Nonlinear model Rn^*_{xz}

Figure 2. Reproducibility check of instantaneous turbulent stress for the flow around a single cylinder ($R_e = 700$)

RESULTS AND DISCUSSIONS

Figure 2 shows instantaneous observed turbulent stress R^*_{xz} and calculated turbulence stress Rs^*_{xz} and Rn^*_{xz} for the flow around a single cylinder. Each values is normalized by approaching velocity V_0. As can be seen in **Figure 2**(a), positive and negative stress R^*_{xz} were distributed nearby separation points on the cylinder symmetrically. After passing around the cylinder, turbulent stress of opposite sign to those upstream values were observed respectively in the wake region.

Reproductive turbulent stress by Smagorinsky model Rs^*_{xz} ($C_s = 0.173$) increased nearby burble points on the cylinder, but their signs were different from the observed R^*_{xz}. On the othr hand, the reproductive turbulent stress by nonlinear model Rn^*_{xz} was in good agreement with observed R^*_{xz} qualitatively in whole measurement region. Model coefficient $C_n = 0.08$ was used, which value was obtained as the optimum value for isotropic homogeneous turbulence from DNS results conducted by Borue and Orszag (1998). These results indicates with clarity the superiority of the nonlinear model for the flow around a single circular cylinder include burble and turbulent wake.

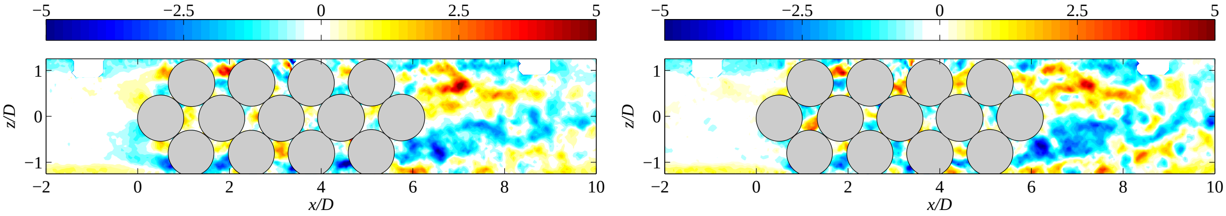

(a) Shear velocity γ^*_{xz} (b) Rotational velocity ω^*_{xz}

Figure 3. Comparison of instantaneous velocity gradient terms (R_{ep}=320, y/D=0.000)

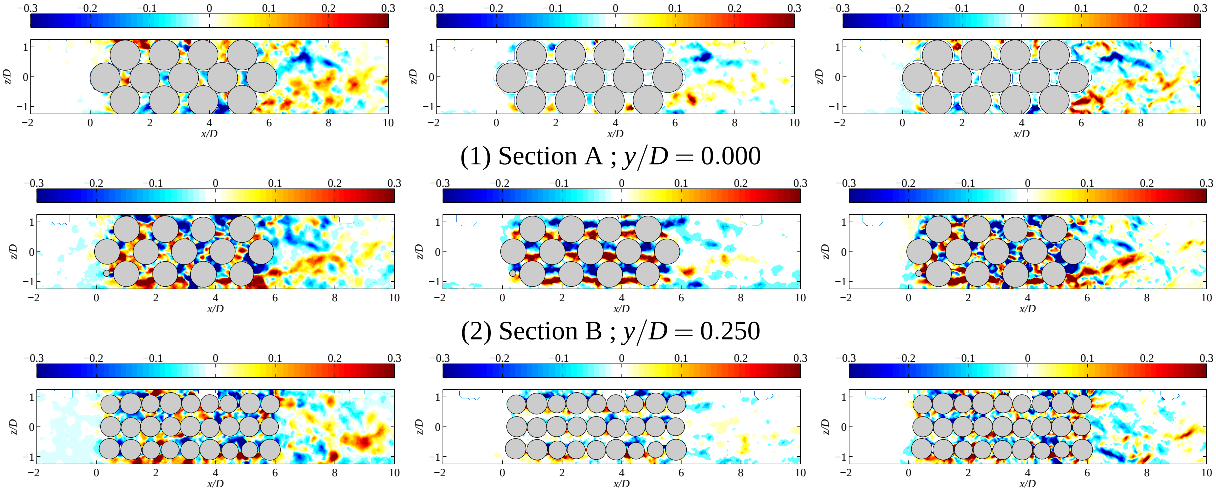

(1) Section A ; $y/D = 0.000$

(2) Section B ; $y/D = 0.250$

(3) Section C ; $y/D = 0.375$

(a) Observed R^*_{xz} (b) Smagorinsky model Rs^*_{xz} (c) Nonlinear model Rn^*_{xz}

Figure 4. Reproducibility check of instantaneous turbulent stress for the flow passing through a porous media (R_{ep}=320)

The following topic is a possibility of omission of the last term in equation (9) for the porous media flow. **Figure 3** shows the example of instantaneous distribution of normalized shear velocity and rotational velocity in porous media flow. It is interesting that shear velocity distribution pattern was similar to that of rotational velocity. This relationship comes out when the velocity gradient $\partial u/\partial z$ is enough larger than $\partial w/\partial x$. If velocity gradient distribution in the plane normal to z-axis, γ_{xy} and ω_{xy}, are similar to that in the plane normal to y-axis, γ_{xz} and ω_{xz}, the relationship $\gamma_{xy} \simeq \omega_{xy}$ is true and virtually the last term in equation (9) is able to be omitted.

Observation of instantaneous normalized turbulent stress at sections ($R_{ep} = 320$) are shown in **Figure 4**(a). Section A ($y/D = 0.000$) was crossing a great circle of central spheres consisted porous media, and in this section, apertures were not connected. Apertures were connected and flow pathway serpentined at section B ($y/D = 0.250$), and there were considerably-straight flow pathway at section C ($y/D = 0.375$). The absolute value of turbulent stress R^*_{xz} was small at upstream of porous media, but it increased drastically just after the flow passed into a porous media. In pores, positive and negative turbulent stress was distributed irregularly at each section and its magnitude was fluctuated. However, from the macroscopic point of view, the mean absolute value was maintained constant value along x-axis in porous media.

As with the flow around a single cylinder, comparison results of reproductive turbulent stress calculated by the Smagorinsky model and the nonlinear model are shown in **Figure 4**(b) and (c) respectively. The Smagorinsky model coefficient was used a value of $C_s = 0.173$ and the nonlinear model coefficient was used a value of $C_n = 0.16$ so that the mean reproducible error $Err^* = |Rn^*_{xz} - R^*_{xz}|$ can have minimum value. As can be seen in **Figure 4**(b), reproductive turbulent stress Rs^*_{xz} distribution pattern in porous media was roughly similar to observation R^*_{xz} at section B and C where the x-axis directional velocity was dominant, but it was too orderly and not in good agreement with observation in detail. Moreover, Rs^*_{xz} had little correspondance with R^*_{xz} at section A where x-axis directional velocity was small. In the wake region, flume scale distribution pattern of reproduction Rs^*_{xz} was little similar to observation at section A where jet like flow was existed behind a porous media, but it was not in good agreement with observation in detail at every section.

On the contrary, it is obvious that reproductive turbulent stress Rn^*_{xz} calculated by nonlinear model was in good agreement with observation in whole measurement region in detail. But the distribution pattern of Rn^*_{xz} was slightly more peaked than observation.

Predominance of the nonlinear model is also shown by joint probability density function between observation R^*_{xz} and reproduction Rs^*_{xz} or Rn^*_{xz} in **Figure 5**. These joint PDF were

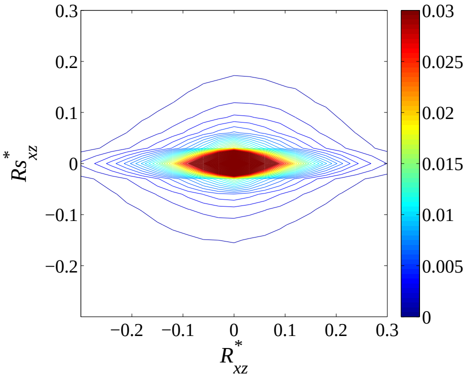

(a) Joint PDF between R^*_{xz} and Rs^*_{xz}

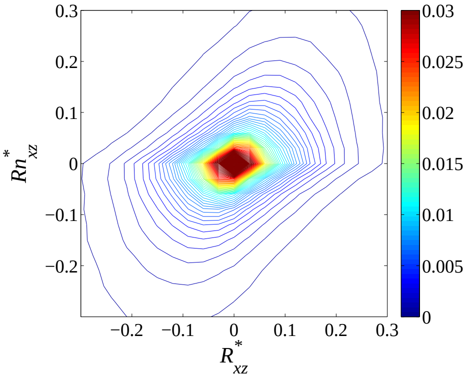

(b) Joint PDF between R^*_{xz} and Rn^*_{xz}

Figure 5. Joint PDF of observed and reproductive turbulent stress in porous media ($R_{ep} = 320$)

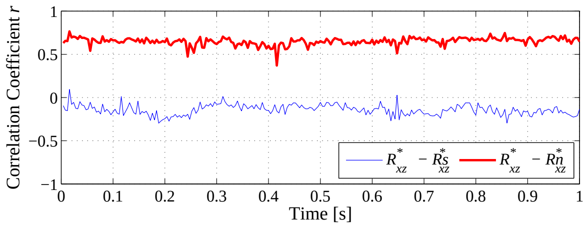

Figure 6. Time series of correlation coefficient between observed R^*_{xz} and reproductive turbulent stress (Smagorinsky model ; Rs^*_{xz}, Nonlinear model ; Rn^*_{xz}, $R_{ep} = 320$)

made from the data in a porous media at all measurement section in $R_{ep} = 320$. The reproduction of the Smagorinsky model Rs^*_{xz} correlate weakly with observation R^*_{xz}, but the reproduction of nonlinear model Rn^*_{xz} had clearly positive linear correlation with R^*_{xz}. **Figure 6** shows time series of spatial correlation between observation and reproductions. Correlation coefficient between R^*_{xz} and Rs^*_{xz} was low and fluctuating, but the one between R^*_{xz} and Rn^*_{xz} was relatively high and almost constant. These relations were not sensitive to the Reynolds number.

The optimum values of model coefficient C_n were decided at each experimental condition in such a way that the mean reproducible error Err^* have minimum value. **Figure 7** is showed the influence of the Reynolds number on C_n. Model

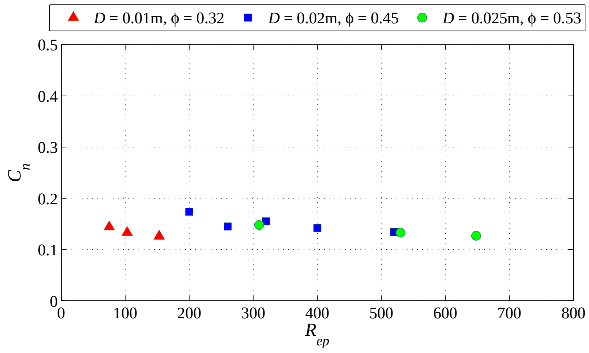

Figure 7. Influence of the Reynolds number on the model coefficient C_n

coefficient was not sensitive to the Reynolds number, and this figure shows also that the mean value of C_n is approximately 0.14. By comparison, Borue and Orszag (1998) derived theoretical model coefficient $C_n = 0.068$ for top-hat filter from Kolmogorov turbulence theory. In addition, they also estimated optimum model coefficient $C_n = 0.08$ from DNS results for the homogeneous turbulence. And Tao *et al*. (2002) estimated model coefficient $C_n = 0.42$ from 3D measurement results for the turbulent jet flow in rectangle duct. These previous information were ensured $C_n = 0.14$ is within reasonable bounds.

Reproducible error Err^* are not able to be identified as the intrinsic error of nonlinear model strictly because it included measurement error. Nevertheless it could estimate that the influence of the Reynolds number on the reproducible error when model coefficient is constant $C_n = 0.14$. Err^* was slightly larger than 0.05 when the Reynolds number was small, but it gradually decreased and was kept below 0.05 with increasing the Reynolds number.

Finally, we confirmed the nonlinear model sensibility to the spatial averaging area size ℓ. Of course, turbulent stress distribution depends on ℓ because the modeling eddy scale is changed. However, the influence of ℓ on the reproducible error Err^* was small. These results indicated that the nonlinear model is robust to the change of ℓ. This robustness was also presented by Borue and Orszag (1998) for the homogeneous turbulence.

CONCLUSIONS

It was examined turbulent stress distribution properties in porous media and suitability of turbulence model based on the velocity information with high resolution measured by using a PTV with RIMM. The following is our conclusions. (1)Preliminary experiment for the flow around a single cylinder showed that the performance of linear eddy viscosity model was not so good, on the other hand, nonlinear model had a potential to reproduce turbulent stress in burble and wake flow in detail. (2)The performance of linear eddy viscosity model was not so good especially at section where X-axis directional velocity was small. And correlation between observation R^*_{xz} and reproduction Rs^*_{xz} was so poor. By contrast, reproduction of nonlinear model Rn^*_{xz} was good agreement with observation even for the 3D flow in porous media, and their correlation was strong. These results clarified an issue for previous turbulence modeling assumed the linear eddy viscosity in porous media. (3)Model coefficient C_n is not so sensitive to the Reynolds number and it kept almost constant value 0.14 in average. And reproducible error Err^* depended on the Reynolds number R_{ep} when R_{ep} was small, but it decreased gradually and was kept below a certain value with increasing of the Reynolds number. (4)Even though modeling turbulent stress depended on the spatial averaging area size ℓ, the influence of ℓ on the reproducible error Err^* was small. This fact shows that nonlinear model was robust to the change of the spatial averaging area size.

REFERENCES

Antohe, B. V., Lage, J. L., 1997, "A general two-equation macroscopic turbulence model for incompressible flow in porous media", Int. J. Heat Mass Transfer, Vol. 40, pp. 3013-3024.

Borue, V., Orszag, S. A., 1998, "Local energy flux subgrid-scale statistics in three-dimensional turbulence", J. Fluid Mechanics, Vol. 366, pp. 1-31.

Clark, R., Ferziger, J. H., Reynolds, W. C., 1979, "Evaluation of subgrid-scale models using an accurately simulated turbulent flow", J. Fluid Mechanics, Vol. 91, pp. 1-16.

Darcy, H., 1856, "Les Fontaines Publiques de la Ville da Dijion, Libraire des Corps Imperiaux des Ponts et Chaussees et des Mines", Dalmont, Paris.

Dill, A. J., Garcia, M. H., Valocchi, A. J., 1995, "Video-based particle tracking velocimetry technique for measuring flow velocity in porous media", Civil Engineering studies Hydraulic Engineering series, No. 48, Illinois Water Resources Center, 89p.

Dybbs, A., Edwards, R. V., 1984, "A new look at porous media fluid mechanics -Darcy to turbulent", Fundamentals of transport phenomena in porous media, pp. 199-254.

Etoh, T., Takehara, T., Yokoyama, Y., Ide, Y., 1996, "Development of supporting technologies for water flow visualization - Density Matching, Refractivity Matching and Multi-Spectrum Measurement" Journal of Hydraulic, Coastal and Environmental Engineering, JSCE, Vol. 566, pp. 84-106.

Jolls, K. R., Hanratty, T. J., 1964, "Transition to turbulence for flow through a dumped bed of spheres", J. Hydraulics Division, Vol. 21, pp.1185-1190.

Liu, S., Meneveau, C., Katz, J., 1994, "On the properties of similarity subgrid-scale models as deduced from measurements in a turbulent jet", J. Fluid Mechanics, Vol. 275, pp. 83-119.

Masuoka, T., Takatsu, Y., 1996, "Turbulence model for flow through porous media", Int. J. Heat Mass Transfer, Vol. 39, pp. 2803-2809.

Nakajo, S., Shigematsu, T., Tsujimoto, G., Takehara, K., 2008, "An experimental study on turbulence induced by porous media", *Proceedings of International Conference of Coastal Engineering*, pp. 4738-4750.

Nakayama, A., Kuwahara, F., 1999, "A macroscopic turbulence model for flow in a porous medium", J. Fluids Engineering, Vol. 121, pp. 427-433.

Pedras, M. H. J., de Lemos, M. J. S., 2001, "Macroscopic turbulence modeling for incompressible flow through undeformable porous media", Int. J. Heat Mass Transfer, Vol. 44, pp. 1081-1093.

Piomelli, U., Moin, P., Ferziger, J. H., 1988, "Model consistency in large eddy simulation of turbulent channel flows", Physics of Fluids, Vol. 31, 1884.

Saleh, S., Thovert, J. F., Adler, P. M., 1992, "Measurement of two-dimensional velocity fields in porous media by particle image displacement velocimetry", Experiments in Fluids, Vol. 12, pp. 210-212.

Tao, B., Katz, J., Meneveau, C., 2002, "Statistical geometry of subgrid-scale stresses determined from holographic particle image velocimetry measurements", J. Fluid Mechanics, Vol. 457, pp. 35-78.

Takehara, K., Adrian, T. J., Etoh, T., 2000, "A proposal of a new Super-Resolution PIV by using the KC method", Annual Journal of Hydraulic Engineering, JSCE, Vol. 44, pp. 431-436.

Teruel, A. E., Rizwan-uddin, 2009, "A new turbulence model for porous media flows. Part I: Constitutive equations and model closure", Int. J. Heat Mass Transfer, Vol. 52, pp. 4264-4272.

Yevseyev, A. R., Nakoryakov, V. E., Romanov, N. N., 1991, "Experimental investigation of a turbulent filtrational flow", Int. J. Multiphase Flow, Vol. 17, pp. 103-118.